Mansoura Engineering Journal

Volume 31 | Issue 2 Article 11

12-14-2020

Modeling Fluidized Bed Combustion of Liquid Fuel.

Farouk Mohamed El-Sayed
Mechanical Power Engineering., Faculty of Engineering., El-Mansoura University., Mansoura., Egypt

MODELING FLUIDIZED BED COMBUSTION OF LIQUID FUEL

نموذج رياضى لإحتراق الوقود السائل فى المهد المميع

Okasha, F.
Department of Mechanical Eng., Faculty of Engineering, Mansoura University, Egypt.
Tel. +20-50-2534382 – Fax. +20-50-2244690
Email: farqokok@mans.edu.eg

ملخص البحث

يلقى حرق الوقود السائل فىالأفران ذات المهد المميع إهتماما متزايدا، خاصة الوقود الثقيل ومخلفات مصافى النفط، إذ أن لهذه الأفران من المرونة ما يمكن من حرق هذه المواد بسلاسة وكفاءة عالية ووفقا للضوابط البيئية. فالإنخفاض النسبى فى درجة حرارة الإحتراق يحد من تكون أكاسيد النيروجين، وإضافة حبيبات الحجر الجيرى يؤدى إلى التخلص من أكاسيد الكبريت.

يهدف هذا البحث إلى بناء نموذج رياضى لمحاكاة إحتراق الوقود السائل فى المهد المميعة. بنى النموذج على أساس نظرية للتميع ذى الطورين المعدلة والتى تفرض أن الغازات تمر خلال المهد فى طورين الأول تلامسى ويمر متخللا الفراغات مابين حبيبات المهد، أما الطور الثانى فعلى هيئة فقاعات. وفى هذا التطبيق يتواجد نوعان من الفقاعات طبقا لمكوناتها الإبتدائية، فالفقاعات المتولدة عند موزع الهواء خالية من الوقود إبتداءً، على عكس الفقاعات المتولدة عند فتحات إدخال الوقود فهى ذات خليط غنى جدا بالوقود منذ البداية، لذا إفترض فى هذا النموذج أن الغازات داخل المهد تتكون من ثلاث أطوار هى تلامسى (emulsion phase) وفقاعات موزع الهواء، وفقاعات الحاقن، كل طور له تكوينه وتفاعلاته ويتبادل مكونات المادة مع الطورين الأخرين.

تم حل معادلات النموذج عدديا بإعداد برنامج فورتران، والذى بواسطتة أمكن الحصول على منحنيات التغير لمكونات الغاز داخل الأطوار الثلاث على طول إرتفاع المهد، كما تم دراسة تأثير عوامل التشغيل المختلفة على أداء عملية الإحتراق. وقد تم أيضا عمل مقارنة مع النتائج العملية التم الحصول عليها للتأكد من مدى صلاحية النموذج حيث وجد توافق جيد.

ABSTRACT

A mathematical model has been developed to predict the combustion of liquid fuel in fluidized bed. From the fluid-dynamic point of view, the model is based on the modified two-phase theory of fluidization where the gas in the bed is assumed to have three phases. A jet-bubble phase which is fuel rich bubbles formed at fuel feeding jet, a distributor-bubble phase which is fuel free bubbles generated at distributor plate and an emulsion phase. Each phase has its composition and exchanges masses with the others two ones.

The bubble is assumed to have a constant size throughout the bed. Gas mixing due to bubbles coalescence is taken into consideration based on an equivalent mass interchange coefficient between the two-bubble phases. The coefficient has been derived based on bubble size growth and probability of coalescence among jet and distributor bubbles.

Two-step fuel reaction has been applied. The fuel firstly reacts to carbon monoxide and water vapor. In the second step, carbon monoxide reacts with oxygen to form carbon dioxide. Mass balance differential equations have been derived for various reacting species (C_xH_y, O_2, CO, H_2O and CO_2) in the three phases. The heavy liquid fuel has been considered as a base case whereas gasoline and diesel fuel have been studied for comparison.

The numerical solution of the model yields the axial concentration profiles of different gaseous species within the three phases. The in-bed fuel combustion has been estimated. The relative importance of gas mixing due to bubble coalescence has been assessed. The influences of different parameters on the combustion performance have been studied and discussed. Among the later parameters, jet velocity has a major effect on combustion performance.

Experimental tests have been carried out to validate the model using a bubbling fluidized bed combustor of 300 mm inner diameter. The comparison between the model and experimental results shows a good agreement, especially, at higher jet velocity.

KEYWORDS

Modelling, Combustion, Fluidized Bed, Liquid Fuel

Accepted June 29, 2006

INTRODUCTION

Recently, fluidized bed combustion of liquid fuels has received more attention; in particular, heavy oil and refinery residues that contain high level of sulfur content. Those fuels can be reliably processed using fluidized bed combustion thanks to its robustness, flexibility and effectiveness [1], whilst meeting environmental standards on pollutant emissions, with particular concern to *in situ* desulphurization. Thanks to the optimization of the operating conditions and a good design of the fuel injection system, a wide range of liquid fuels have been efficiently burned in fluidized beds including acid tar, heavy fuel oil, kerosene, pyrolysis oil, bitumen-based emulsion, gas-oil and asphalt [2-7].

In earlier modeling work on fluidized bed combustion of gaseous and liquid fuels, a diffusion-based plume model was proposed by Stubington and Davidson, [8] and Borodulya et al. [9]. More recently, Miccio et al. [10-13] have given a significant contribution for modeling of combustion of liquid in FB. The modeling development has been centered on the fate of rising fuel vapor bubble as a consequence of reaction, mass and heat transfer. A simplified model for desulphurization of heavy liquid fuel has been proposed by Miccio and Okasha [14]. Okasha and Miccio [15] have developed a model for the interaction of the assisted-air-liquid fuel jet with fluidized bed particles. The model can predict the rate of liquid fuel evaporation inside the jet flare. Moreover, the model can be utilized to estimate the initial concentrations of fuel vapor in bubble and emulsion phases.

The objective of the present paper is primarily to develop a mathematical model for fluidized bed combustion of liquid fuel. The model should have some advantages over the models mentioned above, being a relatively simple and dealing with three interacting phases in a comprehensive way. Therefore, the model pays equal attention for all the three phases and doesn't focus on a certain one as in some models above [8-13]. Further, the model integrates in its structure the prediction of a sub-model [15] that furnishes the initial concentrations of fuel vapor in the phases. The model simulation provides the axial profiles of different species in the three bed phases. In this way, the mechanism of liquid fuel combustion in fluidized bed has been deeply explored by the analysis of the obtained results. Finally, the model results are compared to experiments carried out in a pre-pilot scale fluidized bed combustor.

NOMENCLATURE

A_{fb} bed cross section area, m^2
A_{jo} orifice area of the injector, m^2
C molar concentration, kmole/m^3, except in eqn 35, gmole/cm^3
D molecular diffusion coefficient, m^2/s
d_b bubble diameter, m
d_{bm} average bubble diameter, m
d_c diameter of fluidization column, m
E activation energy of reaction, kcal/gmole
EA Excess air factor
f_{jd} relative frequency of coalescence between the jet and the distributor bubble-phases
g acceleration of gravity, m/s^2
H_{ch} expanded bed height, m
H_{mf} bed height at minimum fluidization, m
K_b equivalent mass interchange coefficient among all bubbles, s^{-1}
K_{bc} coefficient mass interchange between bubble and cloud-wake region, s^{-1}
K_{be} coefficient mass interchange between bubble and emulsion phase, s^{-1}
K_{ce} coefficient mass interchange between emulsion phase and cloud-wake region, s^{-1}
K_{CO} reaction rate constant of carbon monoxide
K_f reaction rate constant of fuel vapor
K_{jd} equivalent mass interchange coefficient between distributor and jet-phases, s^{-1}
M molecular weight, kg/kmole
m_{da} air fed rate through the distributor, kg/s
m_{ja} mass rate of dispersing air fed through jet, kg/s

m_{jb} mass rate of gases included in bubble-jet phase, kg/s
m_f mass rate of liquid fuel fed into the bed through the jet, kg/s
n_{jb} frequency of jet bubbles, s^{-1}
n_{db} frequency of distributor bubbles, s^{-1}
R reaction rate, kmole/(m^3.s)
R_f reaction rate of fuel vapor, eqn. 35, gmole/(cm^3.s)
R_{CO} reaction rate of carbon monoxide, kmole/(m^3.s)
R_μ universal gas constant, kg/(kmole.K)
r_{jfv} mass ratio of liquid fuel vapor released inside the jet flare
T temperature, K
T_b bed temperature, °C
t time, s
u_b bubble rise velocity, m/s
u_{bm} rise velocity of mean bubble, m/s
u_{br} rise velocity of single bubble, m/s
u_e superficial velocity of the gas through the emulsion phase, m/s
u_j dispersing air velocity, m/s
u_{mf} superficial gas velocity at minimum fluidization conditions, m/s
u_o superficial gas velocity, m/s
V_{db} volumetric rate of gases included in distributor-bubble phase, m^3/s
V_b total volumetric rate of the two bubble phases, m^3/s
V_{jb} volumetric rate of gases included in jet-bubble phase, m^3/s
v_b a bubble volume, m^3
v_{bm} mean volume of the bubble through the expanded bed, m^3
Z dimensionless height in the bed
z height in the bed, m

Greek Symbols

ε_{mf} voidage fraction in the emulsion phase at minimum fluidization
ρ_a density of air at bed temperature, kg/m^3
ρ_{ao} density of air at nozzle temperature, kg/m^3.
δ fraction of bed in bubble
δ_{db} fraction of bed in the distributor bubbles
δ_{jb} fraction of bed in the jet bubbles

MODEL FORMULATION

The present model is based on the modified two-phase theory of fluidization. The gases in all bed phases including the emulsion phase are assumed to be in plug flow. The two steps combustion mechanism has been applied. The conservation equations of chemical species are expressed in the three phases considering chemical reactions, mass transfer and bubbles coalescence. Five chemical species (C_xH_y, O_2, CO, H_2O and CO_2) are taken into consideration.

Modified Two Phase Model

According to the two-phase theory of fluidization, the bed is assumed to be comprised of two phases, a bubble phase and emulsion phase. For the present application, there are two types of bubbles based on the source of generation. The first type is the distributor bubbles formed by the air fed through the distributor whereas the second one is the jet bubble created at the pneumatic jet feeding liquid fuel. The two bubbles are different in initial composition. The jet bubbles are usually fuel vapor rich whereas distributor bubbles are initially fuel vapor free. Each type will be treated as independent phase, therefore, the gas inside the bed will be simply considered as three phases, namely, emulsion phase, distributor-bubble phase and jet-bubble phase. The three phases interchange gases among each other.

Emulsion Phase

The superficial gas velocity through the emulsion, u_e, is given by the following expression [16,17] instead of minimum fluidization velocity, u_{mf}.

$$(u_e - u_{mf})/(u_o - u_{mf}) = 1/3 \qquad (1)$$

Jet Bubble Phase

A characteristic of a jet in fluidized bed is the periodical bubble detachment. It is well documented that not all the injected gases are included within the jet bubbles [17,18]. The percentage of injected gas that contributes in forming bubbles has been estimated to be 54%-37% [19, 20]. Yates et al. [21] obtained the percentages for Geldart AB particles as 36% and 79% at height of 10 cm and 25 cm, respectively.

For the present model it is assumed that 50% of the injected air and the fuel vapor released inside the flare is converted into jet bubbles. The remaining half is assumed to leak uniformly through the emulsion phase. The mass rate, m_{bj}, and volumetric rate, V_{bj}, of jet-bubble phase are given, respectively, by,

$$m_{jb} = 0.5 * (m_{ja} + r_{jfv} m_f) \qquad (2)$$

$$V_{jb} = 0.5 * (m_{ja} + r_{jfv} m_f) / \rho_a \qquad (3)$$

where m_{ja} is the rate of dispersing air fed through the jet calculated by

$$m_{ja} = A_{jo} \rho_{ao} u_j \qquad (4)$$

where m_f is the feeding rate of liquid fuel and r_{jfv} is the mass fraction of fuel vapor released inside the jet flare. The later one is estimated using a model developed by Okasha and Miccio [15]. Table 1 reports the ratio of fuel vapor that is released inside the flare for different fuels. A_{jo} is the orifice area of the injector, ρ_a and ρ_{ao} are the density of air at bed temperature and at injection temperature, respectively. u_j is the dispersing air velocity.

The bubble diameter is assumed to be constant throughout the bed and equal to the average bubble taking into account both of fed air and liquid fuel vapor.

The frequency of jet bubbles, n_{jb}, is calculated as the ratio of the volumetric rate of jet bubble to the average volume of the bubble calculated on the base of the expanded bed height, v_{bm}.

$$n_{jb} = V_{jb} / v_{bm} \qquad (5)$$

Table 1. Fuel vapor fraction released inside the flare as a function of injection conditions

u_j	AFR_j	fraction of released vapor inside the jet flare, r_{jfv}		
m/s	-	Heavy Fuel	Diesel	Gasoline
20	0.466	0.034	0.452	0.687
40	0.932	0.248	0.774	0.934
60	1.398	0.485	0.974	0.999
80	1.863	0.685	0.999	1.00
100	2.329	0.842	1.00	1.00
120	2.795	0.923	1.00	1.00
140	3.26	0.962	1.00	1.00
160	3.727	0.982	1.00	1.00
180	4.19	0.999	1.00	1.00
200	4.658	1.00	1.00	1.00

Distributor Bubble Phase

As recognized by Hilligardt and Werther [16]; and Kunii and Levenspiel [17] not all excess gas, $u_o - u_{mf}$, passes through the bed as observable bubbles. They reported that about 65% of the excess gas flows as bubble for Geldart B. The distributor-bubble phase volumetric rate, V_{db}, is estimated to be:

$$V_{db} = (u_o - u_e) A_b - V_{jb} \qquad (6)$$

The superficial velocity of gases, u_o, is calculated as

$$u_o = (m_{da} + m_{ja} + m_f) / (A_B \rho_a) \qquad (7)$$

where m_{da} is the air feeding rate through the distributor plate.

The frequency of distributor bubbles, n_{db}, is given by

$$n_{db} = V_{db} / v_{bm} \qquad (8)$$

Bubble Diameter

It is assumed that the two-bubble phases have the same constant bubble size through the bed height equal to the average bubble size. The equation given by Cai et al. [22] has been used to estimate the bubble diameter, d_b.

$$D_b = 0.38 * H^{0.8}(U - U_{mf})^{0.42} * \exp[-0.25(U - U_{mf})^2 - 0.1(U - U_{mf})] \quad (9)$$

The average bubble diameter, d_{bm}, in the whole bed is obtained by integrating the equation along the expanded bed height.

$$\tilde{D}_b = 0.21 * H_f^{0.8}(U - U_{mf})^{0.42} * \exp[-0.25(U - U_{mf})^2 - 0.1(U - U_{mf})] \quad (10)$$

Bubble Rise Velocity

The bubble rise velocity, u_b, is estimated by an equation due to Davidson and Harrison [23]

$$u_b = (u_o - u_{mf}) + u_{br} \quad (11)$$

where u_{br} may estimated as proposed by Kunii and Levenspiel [17]:

$$u_{br} = 0.711(gD_b)^{1/2} \qquad d_b/d_c<0.125 \quad (12)$$

$$u_{br} = [0.711(gD_b)^{1/2}] * 1.2\exp(-1.49\frac{D_b}{d_t}) \qquad 0.125<d_b/d_c<0.6 \quad (13)$$

$$u_{br} = 0.35(gD_b)^{1/2} \qquad d_b/d_c>0.6 \quad (14)$$

Bed Expansion and Fraction of Bed in Bubbles

For solids of Geldart B, the emulsion phase voidage remains very close to ε_{mf}, so that bed expansion arises entirely from the volume occupied by bubbles, δ, [24], i.e.,

$$(H_{eb} - H_{mf})/H_{eb} = \delta \quad (15)$$

where H_{eb} and H_{mf} are the expanded bed height and bed height at minimum fluidization, respectively.
The total bubble flow can be written as

$$V_b = \delta u_{bm} A_b = (u_o - u_e) A_b \quad (16)$$

Combining between the above two equations, the following expression can be obtained.

$$\frac{H_{eb} - H_{mf}}{H_{eb}} = \delta = \frac{u_o - u_e}{u_{bm}} \quad (17)$$

To estimate bed expansion and average bubble size an iterative method is used to solve equations 10 and 17. Accordingly, the velocity of average size bubble, expanded bed height and fraction of bed in bubbles can be determined.
The fraction of distributor bubbles, δ_{db}, and jet bubbles in bed, δ_{jb}, can be given as:

$$\delta_{db} = (V_{db}/V_b)\delta \quad (18)$$

$$\delta_{jb} = (V_{jb}/V_b)\delta \quad (19)$$

Mass Transfer between the Bubble and Emulsion Phases

The mass transfer coefficient between bubble and emulsion phase is determined using the correlations reported by Kunii and Levenspiel [17].

$$(1/K_{bc}) = (1/K_{bc}) + (1/K_{ce}) \quad (20)$$

$$K_{bc} = 4.5\frac{u_{mf}}{d_b} + 5.85\frac{D^{1/2}g^{1/4}}{d_b^{5/4}} \quad (21)$$

$$K_{ce} = 6.78(\varepsilon_{mf} D u_b / d_b^3)^{1/2} \quad (22)$$

Mass Interchange between Distributor and Jet Bubble Phases

It is well known that bubble size in fluidized bed grows with height above the distributor whereas the bubble frequency decreases. This phenomenon is mainly attributed to bubbles coalescence. Jet in fluidized beds is another source of bubbles other than the gas distributor. Whenever compositions of the two bubbles types are different, gas mixing due to coalescence should have a significant effect on chemical processes. So it is important to quantify gas mixing due to the coalescence between the two types of bubbles. In the following an approach is proposed to deal with a typical case established in fluidized bed combustors burning liquid fuel fed by a pneumatic injector.

In the present model it is assumed that the bubble has a constant size through the bed, and hence, the bubbles coalescence and the consequent mixing of their constituents could be missing. The gas mixing due to bubbles coalescence, however, is taken into account by converting the bubble growth into an equivalent mass interchange rate between the two types of bubbles while maintaining the assumption of constant bubble size.

The volume of bubble with diameter d_b at height z is determined as:

$$v_b = (\pi/6)d_b^3 \tag{23}$$

The change of bubble volume with height is

$$\frac{dv_b}{dz} = (\pi/2)d_b^2\frac{dd_b}{dz} \tag{24}$$

The rate of change in bubble volume can be written as:

$$\frac{dv_b}{dt} * \frac{dt}{dz} = (\pi/2)d_b^2\frac{dd_b}{dz} \tag{25}$$

Replacing $\frac{dz}{dt}$ with bubble rising velocity, u_b, in the above equation

$$\frac{dv_b}{dt} = (\pi/2)d_b^2\frac{dd_b}{dz}u_b \tag{26}$$

Dividing by volume of bubble, the rate of bubble size increment based on a unit volume is given as

$$K_b = 3\frac{u_b}{d_b}\frac{dd_b}{dz} \tag{27}$$

K_b may be considered as an equivalent mass interchange coefficient among all bubbles that is counterpart to the rate of gas mixing due to bubble coalescence.

If it is assumed that the coalescence among all bubbles is equally likely, then the relative frequency of coalescence among the jet bubbles and the distributor bubbles to the total frequency of bubbles coalescence can be expressed as,

$$f_{jd} = \frac{2n_{db}n_{jb}}{(n_{db}+n_{jb})(n_{db}+n_{jb}-n_1)} \tag{28}$$

where $n_1 = 1 \ s^{-1}$. Considering the assumption that the bed has a uniform bubble size and using equationns 5 and 8, the above expression may have the following form

$$f_{jd} = \frac{2V_{db}V_{jb}}{(V_{db}+V_{jb})(V_{db}+V_{jb}-n_1 v_{bm})} \tag{29}$$

The equivalent mass interchange coefficient between distributor and jet bubbles based on unit volume of all bubbles, K_{jd} may given as

$$K_{jd} = 3f_{jd}(u_b/d_b)(dd_b/dz) \tag{30}$$

Initial Concentration of Fuel Vapor in Phases

The study carried out on the pneumatic feeding of liquid fuel in fluidized bed [15] showed that fuel, partially or even totally, evaporates inside the jet flare depending on injection conditions and fuel type. According

to the justification mentioned above it is assumed that 50% of fed air and fuel vapor released inside the jet flare are going to form jet bubbles. The remaining part of air and fuel vapor is assumed to leak uniformly through the emulsion phase. Moreover, the part of fuel reaches the jet boundaries in liquid state is considered to evaporate uniformly through the emulsion phase. As discussed below, the liquid fuel is assumed to release as hydrocarbon (C_xH_y).

The distributor bubble is initially assumed to be fuel vapor free, at distributor level.

$$C_{C_xH_y,db,o} = 0 \qquad (31)$$

The initial concentration of fuel vapor in jet-bubble phase is given by:

$$C_{C_xH_y,jb,o} = \frac{r_{jfv} m_f}{M_{C_xH_y} * [(m_{ja} + r_{jfv} m_f)/\rho_a]} \qquad (32)$$

The initial concentration of fuel vapor in emulsion phase is calculated as

$$C_{C_xH_y,e,o} = \frac{m_f (1 - 0.5 * r_{jfv})}{(M_{C_xH_y} * u_e * A_b)} \qquad (33)$$

Kinetics of Liquid Fuel Combustion

Seeking for simplicity, two-step fuel reaction has been applied [25]. The fuel primarily reacts to carbon monoxide and water vapor. The rate of hydrocarbon conversion is determined by an expression developed by Westbrook and Dryer [26].

$$C_xH_y + 1/2(x + y/2)O_2 \rightarrow xCO + \frac{y}{2} H_2O \qquad (34)$$

$$R_f = k_f [C_{C_xH_y}]^a [C_{O_2}]^b \qquad (35)$$

where

$$k_f = A.\exp[-E/R_\mu T] \qquad (36)$$

Three liquid fuels have been considered in the present study. They are Gasoline, Diesel and a heavy fuel that are simply represented by n-octane, n-dodecane and n-heptadecane as pure hydrocarbons. Table 2 reports their corresponding properties and constants.

In the second step carbon monoxide reacts with oxygen to form carbon dioxide. The expression developed by Howard et al. [27] is used to calculate the rate of the latter reaction.

$$CO + (1/2)O_2 \rightarrow CO_2 \qquad (37)$$

$$R_{CO} = k_{CO}[C_{CO}][C_{H2O} C_{O2}]^{1/2} \qquad (38)$$

where

$$k_{CO} = 1.3.10^{11}.\exp[-15088/T] \qquad (39)$$

Table 2. Properties and constants of the fuels

fuel	n-octane	n-dodecane	n-heptane
formula	C_8H_{18}	$C_{12}H_{26}$	$C_{17}H_{36}$
molecular weight	114.23	170.33	240.46
boiling temp., °C	126	216	302
a	0.25	0.25	0.25
b	1.5	1.5	1.5
A, gmole/cm³s	$5.7*10^{11}$	$3.9*10^{11}$	$2.3*10^{11}$
E, kcal/gmole	30	30	30

Fundamental Equations: Differential Species Balances

When dealing with combustion kinetics, five species have been taken into consideration that include released fuel vapor as hydrocarbon, C_xH_y, oxygen, O_2, water vapor, H_2O, carbon monoxide, CO and carbon dioxide, CO_2. Referring to Fig. 1 the mass differential balances of the species have been derived making the following assumptions:

- The bed has three phases: emulsion, distributor-bubble and jet-bubble
- Gas is in plug flow in the three phases
- Gas interchange takes place among the three phases
- The bubble size is uniform in the bed and equal between jet and distributor-bubble phase
- All the bubbles start traveling at the distributor plate
- The three phases have uniform temperature, namely bed temperature.

- The fuel vapor releases in jet-bubble and in emulsion-phase.
- CO oxidation rate (38-39) is reduced by a factor 0.1 (Philippek et al., 1997) to account for surface radical deactivation in emulsion phase.

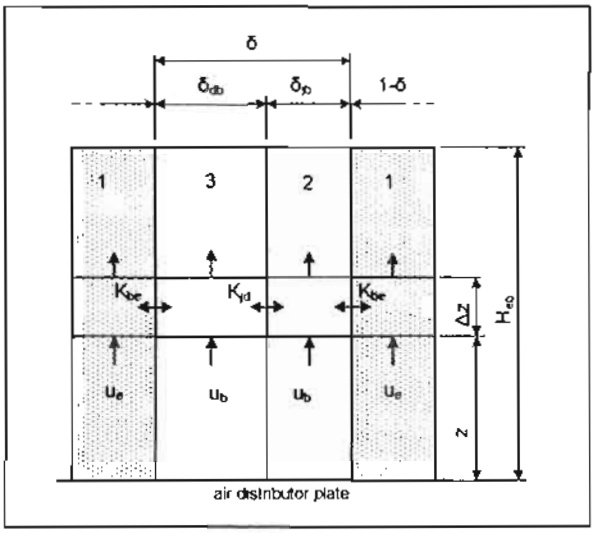

1. emulsion phase, 2.jet bubble phase, 3. distributor bubble phase

Fig. 1. Schematic of the model

In the differential equations, the vertical position in the bed is made dimensionless dividing by the expanded bed height, $Z = z / H_{eb}$.

Mass balance of species i in jet bubble phase,j,

$$\frac{dC_{j,i}}{dZ} = \frac{H_{eb}}{u_b}(\sum R_i) + \frac{H_{eb}K_{dj}\delta}{u_b\delta_j}(C_{d,i} - C_{j,i}) + \frac{H_{eb}K_{be}}{u_b}(C_{e,i} - C_{j,i}) \quad (40)$$

Mass balance of species i in distributor bubble phase, d,

$$\frac{dC_{d,i}}{dz} = \frac{H_{eb}}{u_b}(\sum R_i) + \frac{H_{eb}K_{dj}\delta}{u_b\delta_d}(C_{j,i} - C_{d,i}) + \frac{H_{eb}K_{be}}{u_b}(C_{e,i} - C_{d,i}) \quad (41)$$

Mass balance of species i in emulsion phase, e,

$$\frac{dC_{e,i}}{dz} = \frac{H_{eb}\varepsilon_{mf(1-\delta)}}{u_e}(\sum R_i) + \frac{H_{eb}K_{be}\delta_d}{u_e} * (C_{d,i} - C_{e,i}) + \frac{H_{eb}K_{be}\delta_j}{u_e}(C_{j,i} - C_{e,i}) \quad (42)$$

In the latter equations, the first term of the right hand side accounts for the sum of generation and consumption of i^{th} component due chemical reaction. The second term in Eqs 40 and 41 represents the interchange of gas between the two bubble phases due to bubble coalescence. The remaining terms express the exchange of gases between emulsion and the two bubble phases.

Numerical Computations

Numerical solution of the 15 differential equations (40-42) has been realized using a fourth order Runge-Kutta method. The calculations were carried out using a Pentium III PC. Since the beginning the results clearly indicated that the variation rates of species concentrations are very high close to the distributor then decrease with bed height. Therefore, the integration step has been chosen very small in the lower part of bed and then it is gradually increased with bed height.

RESULTS AND DISCUSSION

The proposed model developed above has been solved to predict the axial variation of species mole fraction along the bed height. Moreover, the influences of different parameters on the combustion processes have been evaluated. A comparison with experimental results is also given. An attention is first given to the interchange of gases between the two bubble phases due to their coalescence. In the following discussion the phase-averaged mole fraction is introduced as the sum of the moles of a certain species in the three phases divided by the total moles of all species.

Gases Interchange between the Two Bubble Phases

The equivalent mass interchange coefficient between distributor- and jet-bubble phase, K_{jd}, has been calculated and presented in Fig. 2 as a function of the height in the bed. The coefficient has very high values close to the distributor, i.e. about 70 s^{-1}; then it gradually decreases down to 0.26 s^{-1} at the bed surface. This trend is consistent since the growth rate of bubble size is higher in the lower part of the bed. At Z≈0.25, K_{jd} takes a value that is comparable to the mass transfer coefficient between bubble and emulsion phases (i.e., around 1.0 s^{-1}) under a base case conditions, where u_j=80 m/s, T_B=850 °C, EA=1.1 and u_o=1.0 m/s. Heavy fuel is considered for the base case as fuel type.

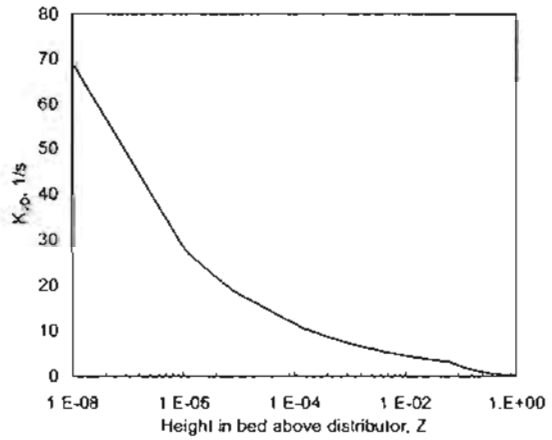

Fig. 2. Equivalent interchange coefficient between distributor- and jet-bubble phases

Axial Variation of Species Concentrations along the Bed Height

The axial variations in species mole fraction within the different phases have been estimated using the developed model discussed earlier. The obtained results are illustrated in Figs 3 and 4. The results have been estimated for two cases, i.e., considering and neglecting ($K_{jd} = 0$) the interchange of gases between the two bubble-phases. The comparison between the two cases demonstrates the impact of K_{jd} on the model results. The calculations are carried out under the base case conditions.

Figure 3.a shows the axial variation in mole fraction of fuel vapor within the different phases. As shown in the figure, the concentrations of fuel vapor in the two bubble phases immediately drop close to zero when considering K_{jd}, denoted by black symbols. It appears that the combustion processes in bubble phases are under a chemical kinetic control as the oxygen required for reaction is available (see Fig. 3.c). The initial concentration of fuel vapor in jet-bubble phase is very high (very rich mixture); however, the gas interchange due to bubbles coalescence is so fast that it brings the concentrations in the two bubble phases to the average one through a very short distance. On the other side, looking at to the emulsion phase profile with symbol of black circles, it is noted that a great part of fuel vapor (about 90% under the present considered conditions) oxidizes through a small part of bed height, Z≈0.1. As shown in Fig. 3.c, along this distance, close to the distributor, O_2 in emulsion remains available and the chemical kinetics still controls the reaction. To this end, the oxygen concentration falls to a very low value and the reaction becomes under a mass transfer control. Although the bubble phases are still O_2 rich, the oxygen is transported with small rate as the mass transfer between the emulsion and the bubble phases is relatively slow. Consequently, the rate of fuel conversion greatly lessens, and hence, a part of fuel vapor in emulsion phase may navigate the bed without conversion.

Alternatively, when neglecting the interchange of gas between the two-bubble phases ($K_{jd} = 0$), the plots are referred by open symbols. For first glance, it is recognized that the highest impact meets the jet-bubble phase. The reaction rate of fuel vapor inside the phase greatly reduces due to the lack of oxygen. As shown in Fig. 3.c, the oxygen in jet-bubble phase is rapidly consumed as the initial mixture within the phase is highly rich with fuel vapor. At Z≈0.08, the rate of fuel conversion greatly reduces to a constant value as the mole fraction has a linear trend. In fact, the process turns into mass transfer controlled as it is mainly based on mass exchange

(oxygen and fuel vapor) with the distributor-bubble phase via the emulsion phase. Obviously, a great part of fuel vapor inside the jet-bubble phase reaches the bed surface without conversion. On the other hand, the concentration of fuel vapor in emulsion phase slightly increases. This latter should be also ascribed to the shortage of oxygen in jet-bubble phase. In fact, jet-bubble phase becomes a sink rather than a source of oxygen while it exchanges gases with the emulsion phase and vice versa when considering fuel vapor (see figures 3.a and 3.c). In Fig.s 4.a and 4.b, phase-averaged mole fraction of different species has been presented as a function of height above distributor. As shown in Fig. 4.a, the phase-averaged mole fraction of fuel vapor considerably increases when neglecting K_{jd}. It turns out to be 0.0013 instead of 0.00008, i.e., it multiplies about 16 times.

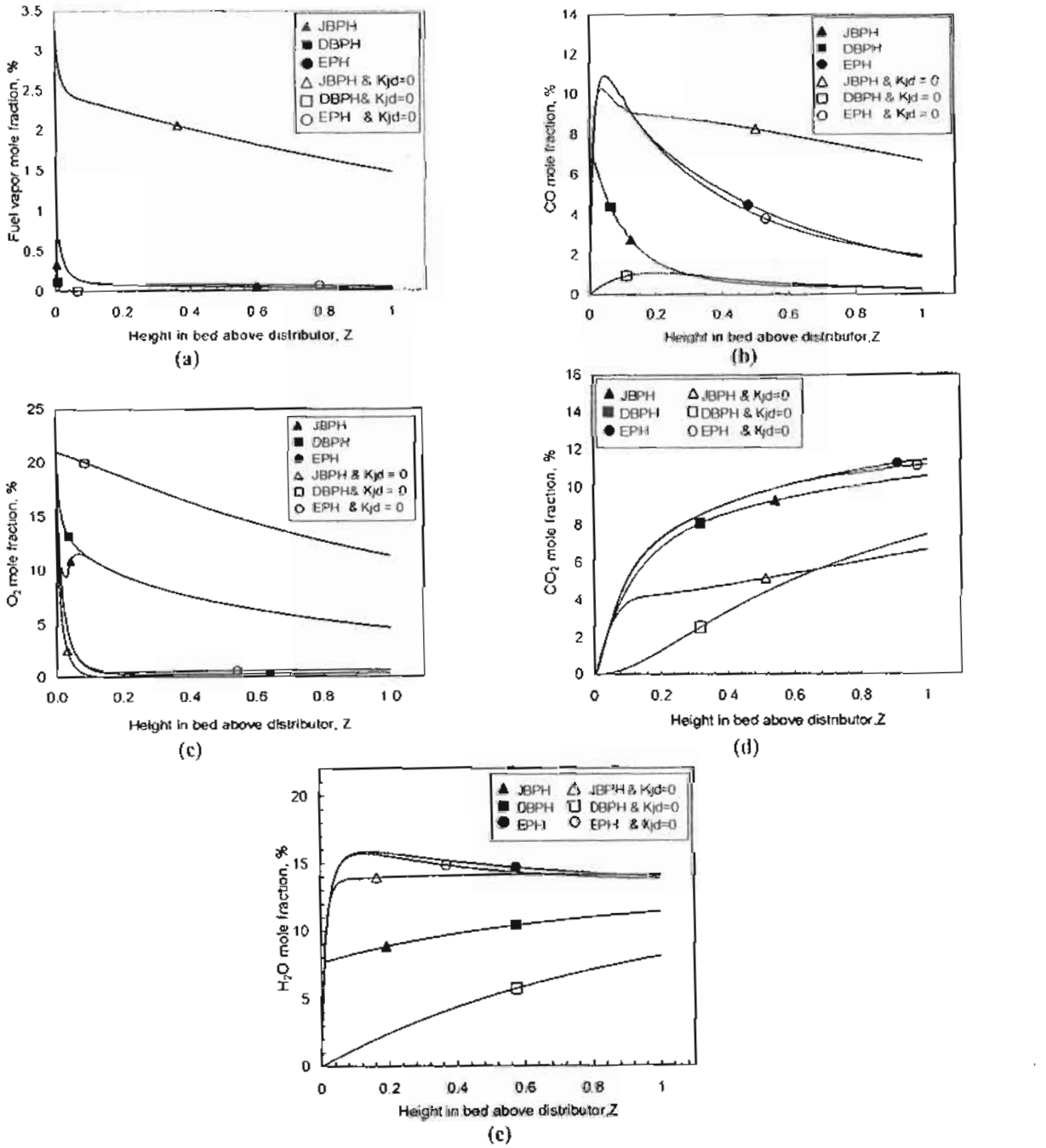

Fig. 3. Axial concentration profiles of different species in the bed phases

Figure 3.b illustrates the axial profiles of mole fraction of the carbon monoxide in different phases. It is obvious that the CO concentration profile is characterized by a maximum value since CO is generated due to fuel vapor oxidation and subsequently consumed as it oxidized to carbon dioxide. The maximum is more pronounced in the two-bubble phases when considering the gas interchange between them. The results should be attributed to the availability of oxygen, as discussed above that intensifies the chemical reaction. This latter is valid for oxidation of fuel vapor before the peak and for reduction of CO after it. On the other side, the concentration of CO in emulsion phase reaches the maximum somewhat later. The rate of fuel vapor conversion in emulsion phase is slightly slower since the oxygen concentration is lower than the average value in the two bubble-phases (see Fig. 3.c). After the maximum, CO concentration gradually diminishes due to the reaction with the remaining portion of oxygen as well as a part transferred from the two-bubble phases. On the other side, a part of CO is transported to the bubble phases due to the concentration difference. Altogether, CO in emulsion phase reaches the bed surface with a mole fraction of about 0.018 that is significantly higher than the corresponding value of the two-bubble phases (about 0.0023).

In the case of neglecting the bubbles coalescence i.e. $K_{jd} = 0$, the profile of CO in emulsion phase is still almost the same (see the two profiles of open and black circle symbols in Fig. 3.b). On the other side, the maximum of CO concentration becomes less pronounced in the two bubble phases, particularly, in distributor-bubble phase. The results should ascribe to the imbalanced initial mixing ratio of oxygen and fuel vapor in the two bubble phases while the mixing due to coalescence is neglected. In fact, the jet-bubble phase initiates fuel very rich while the distributor phase is fuel free. Under these conditions, the conversion processes mainly turn out mass transfer controlled. Since the mass transfer is slow, CO in jet-bubble phase reaches the bed surface with high concentration. Consequently, the phase-averaged mole fraction of CO at bed surface increases to about 0.0149 instead of 0.0093 when considering the gas interchange between the two-bubble phases (see Fig. 4.b).

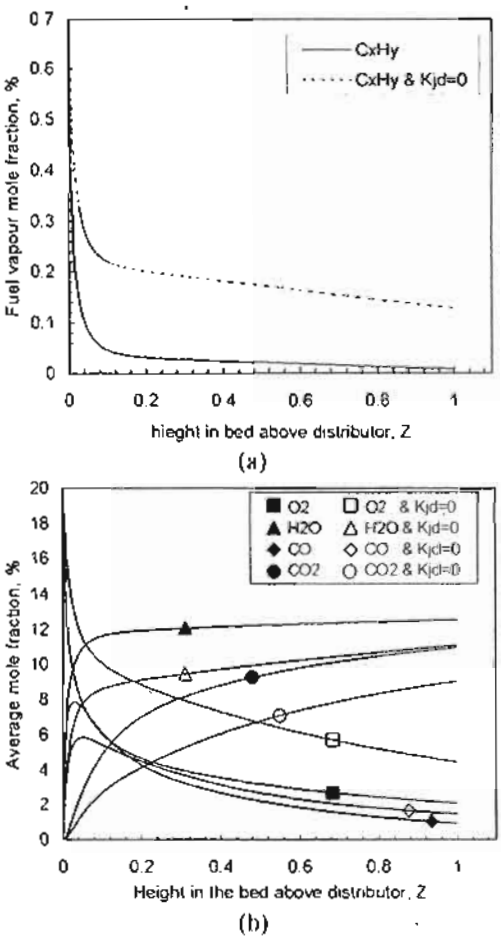

Fig. 4. Axial phase-Averaged concentration of different species in the bed
(Heavy oil, u_j=80 m/s, u_o=1.0 m/s, T_B=850°C & EA=1.1)

The axial profiles of H_2O and CO_2 concentration within the three phases are plotted in figures 3.d and 3.e. CO_2 concentrations have higher values in all phases when considering K_{jd} contribution. H_2O concentrations exhibit a parallel similar trend with the exception emulsion phase. In fact, H_2O is formed just in one step according to Eq. 34, and hence its concentration rapidly grows within the emulsion phase attaining a maximum value, and then reduces due to mass exchange with other phases. Altogether, the averaged-phase concentrations of CO_2 and H_2O increase when considering the K_{jd} contribution, as shown in Fig. 4.b. This result should be ascribed to the better mixing

between combustibles and oxygen in the different phases, in particular, in the two bubble phases.

The above results indicate that the bubbles coalescence phenomenon greatly improves the in-bed combustion processes of liquid fuels, in particular, in the two bubble phases.

Influence of Fluidization Velocity

The influence of fluidization velocity, u_o, on the phase-averaged mole fraction of carbon monoxide is shown in Fig. 5. It is obvious that the peak value of CO is more pronounced at lower fluidization velocity. The lower fluidization velocity consents longer time for fuel vapor reaction resulting in higher concentration of CO. On the other side, the decline of CO profile is faster at lower u_o because of two reasons. First, the rate of carbon monoxide oxidation to carbon dioxide intensifies with the higher H_2O concentration (see Eq. 38). Second, the CO production rate in this stage is lower since larger quantity of fuel vapor is converted in the previous stage. It is also noted that the averaged-phase CO concentration at the bed surface is greater at higher fluidization velocity. Figure 6.a confirms this result where the averaged-phase CO concentration at the bed surface is given as a function of fluidization velocity. Additionally, Fig. 6.a shows that increasing the jet velocity can counterbalance the previously mentioned unfavorable result. At a constant fluidization velocity, increasing jet velocity better regulates the fuel distribution between the emulsion and the bubble phases (see table 3). As a consequence, being mixing more effective, the reaction processes become more intensive as the controlling step in the overall combustion mechanism tends to shift from mass transfer to oxidation kinetics.

Figure 6.b. presents the effect of fluidization velocity on the average concentrations of fuel vapor for different jet velocity. The concentration of fuel vapor is zero for jet velocities 120 and 160 m/s over the considered range of fluidization velocity. The figure also illustrates that the higher fluidization velocity results in increasing fuel vapor concentration at bed surface. The impact turns out to be lower at higher values of jet velocity. The same justifications given for CO trends should be valid for fuel vapor as well.

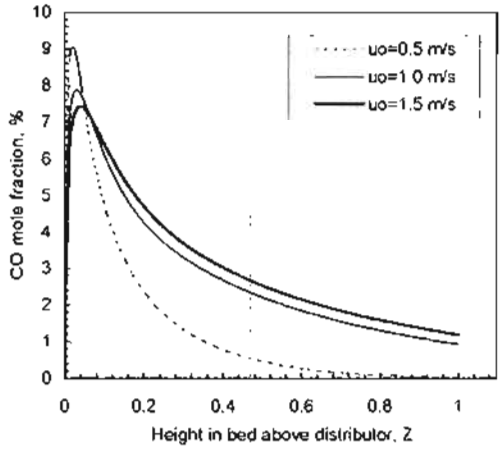

Fig. 5. Axial phase-averaged concentration profile of CO as a function of fluidization velocity
(Heavy fuel, u_j=80 m/s, T_B=850°C and EA=1.1)

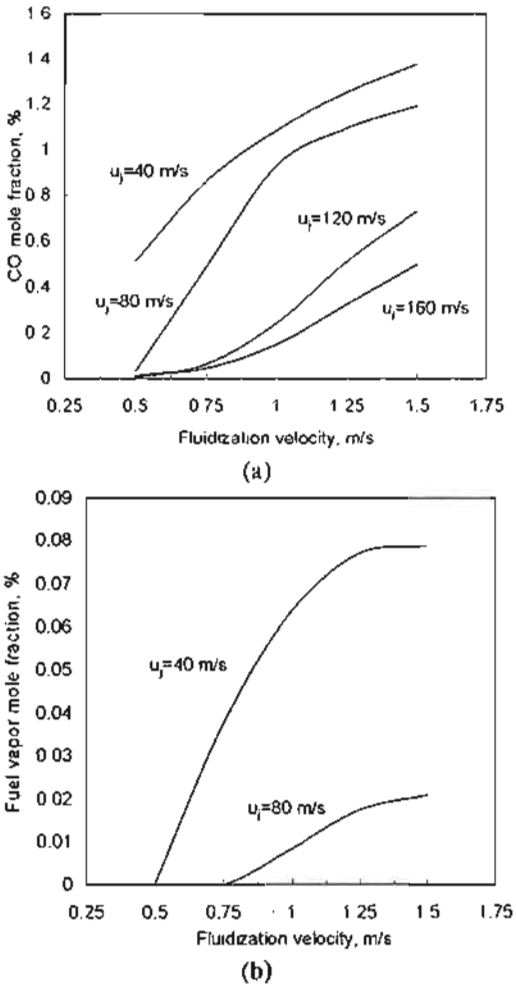

Fig. 6. Influence of fluidization velocity on phase-averaged concentration of CO and fuel vapor

Influence of Bed Temperature

The influence of bed temperature on the phase-averaged mole fraction of fuel vapor and carbon monoxide at the bed surface is presented in figures 7.a and 7.b, respectively. The results are plotted for different u_j. In Fig. 7.a, the fuel vapor concentration at the bed surface is zero for jet velocities 120 and 160 m/s over the considered range of bed temperature. As discussed earlier, at higher jet velocity, the fuel vapor is better distributed between the emulsion and the two bubble phases as reported in table 3 that enhances the combustion processes. On the other side, at lower jet velocity (i.e., u_o=40 and 80 m/s), some fuel vapor reaches the bed surface without conversion. Further, figure 7.a shows that rising the bed temperature slightly increases the fuel vapor concentration at bed surface. On the contrary, CO concentration diminishes with increasing bed temperature as shown in figure 7.b. The reduction rate of CO with temperature is significant in the lower temperature range (i.e., less than 850 °C); however, it becomes less relevant in the higher temperature range.

As a whole, the in-bed combustion significantly improves with bed temperature, especially in the lower temperature range in spite of the increase of fuel vapor concentration with T_B. This unexpected trend could be explained with referring to Fig. 8 where the axial variations of phase-averaged concentration of CO, O_2 and fuel vapor are plotted for two different bed temperatures. Figure 8.a shows that the peak of CO concentration is steeper at higher bed temperature, i.e. T_B=900 °C. The profile indicates that both the formation and reduction rates of carbon monoxide are greater at higher bed temperature. On one side, as it is well known, increasing the temperature intensifies the fuel vapor reaction producing higher rates of H_2O and CO. On the other side, the conversion rate of carbon monoxide to CO_2 intensifies for three reasons: increase of bed temperature, increase of H_2O concentration and increases of CO concentration as well (see Eq.38). Correspondingly, the oxygen consumption rate increases with the bed temperature, as shown in Fig. 8.b. The falling in oxygen concentration in the upper bed part results in lessening the fuel vapor conversion rate. Figure 8.c confirms this trend, i.e., the drop in fuel vapor concentration at T_B= 900 °C is relatively faster in the lower part of bed, where O_2 is still available and the temperature has a higher impact on reaction rate. At a certain height the O_2 concentration becomes so low that its impact overcomes that of the temperature. To this end, the fuel conversion rate at T=800 °C turns out to be greater than that at 900 °C since the corresponding phase-averaged O_2 concentration remains higher. This is demonstrated by the crossing point that the profiles of phase-averaged concentrations of fuel vapor exhibit at Z≈0.2 in Fig. 8.c. As a consequence, the fuel vapor concentration at higher temperature terminates at the bed surface with a greater value.

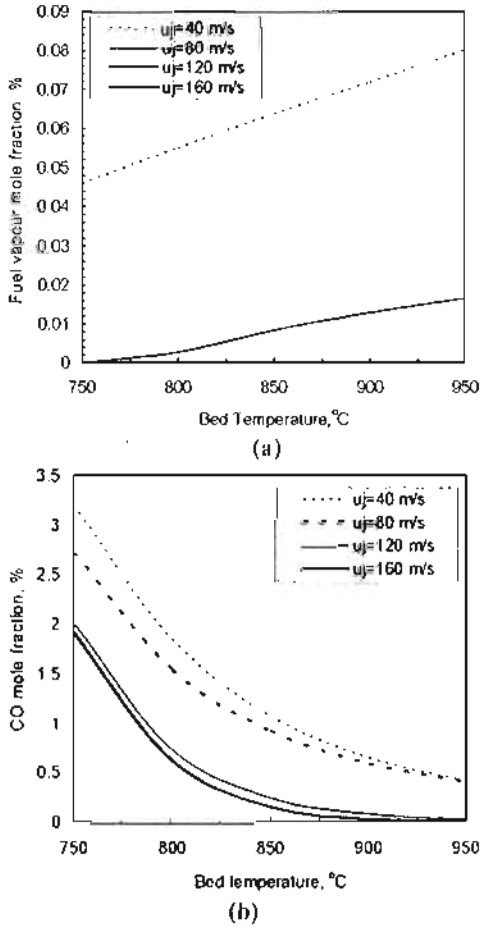

Fig. 7. Influence of bed temperature on phase-averaged concentration of fuel vapor and CO at bed surface for different jet velocities

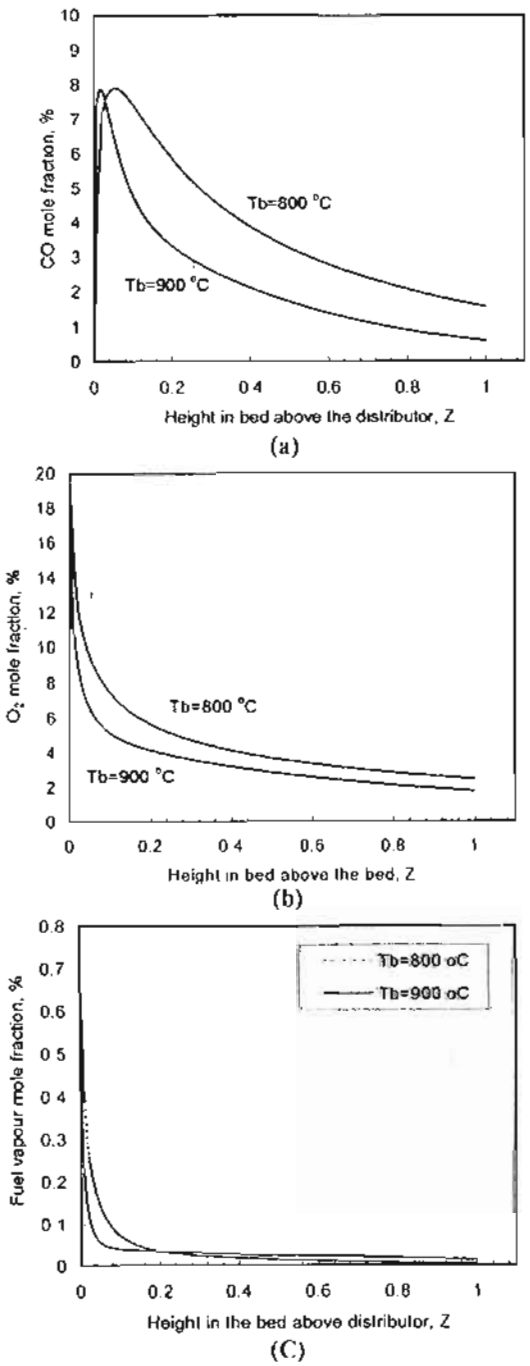

Figure 8. Axial phase-averaged concentration profile of CO, O_2 and fuel vapor at two different temperatures

(Heavy fuel, u_j=80 m/s, u_o=1.0 m/s and EA=1.1)

Influence of Excess Air

The influence of excess air on the combustion of liquid fuel inside the bed has been estimated and presented in figures 9.a and 9.b. Increasing excess air reduces the phase-averaged mole fraction of fuel vapor at bed surface as shown in figure 9.a. The concentrations still diminish with higher jet velocity. The fuel vapor completely disappears for the jet velocities 120 and 160 m/s over the considered excess air range.

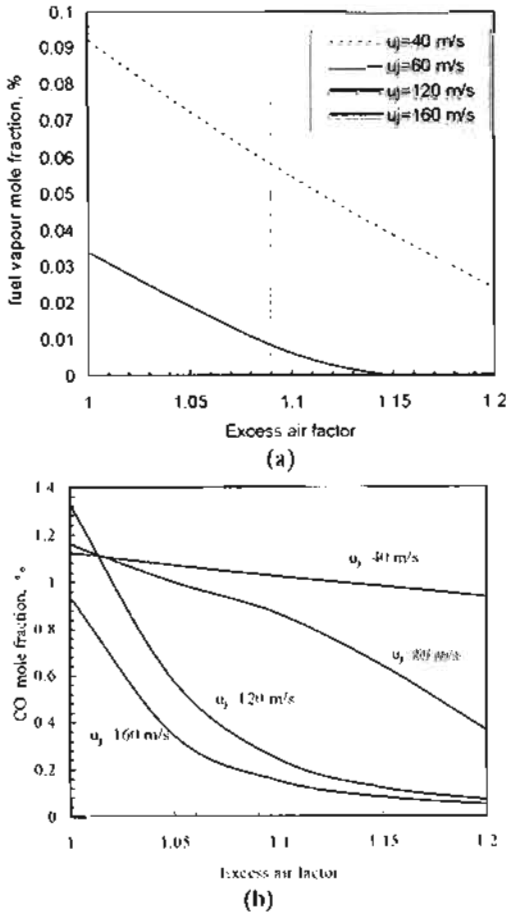

Fig. 9. Influence of excess air on phase-averaged concentration of fuel vapor and CO at bed surface for different jet velocities

Figure 9.b shows the average concentration of carbon monoxide at the bed surface as a function of excess air and jet velocity. As it may be expected the concentration of carbon monoxide decreases with excess air increase. The impact of excess air is high at higher jet velocities (120, 160 m/s). As documented by the data in table 3, the fuel vapor and oxygen are more segregated among the emulsion and the bubbles at lower u_j whereas they are initially better distributed among the phases at higher u_j. Thus, the overall combustion mechanism becomes less dependent on mass transfer control. Therefore, increasing excess air greatly improves in-the bed burning of CO. At excess air greater than 1.15, the effect becomes minor. On the other side, in the case

of smaller jet velocity, increasing excess air has slight effect on carbon monoxide concentration. The mass transfer has a more significant role since the fuel vapor is initially more concentrated at emulsion phase. At moderate u_j, the influence is moderate along the whole range of excess air.

Tab. 3. Initial and final concentrations of fuel vapor (C_xH_y)and oxygen (O_2)
(EA=1.0, u_o=1.0 m/s, T_B=850 °C & Heavy Fuel)

	Average of the two bubble phases			
Species	C_xH_y, ppm		O_2, ppm	
u_j, m/s	initial	final	initial	final
40	1690	0	207081	52078
80	4669	0	201898	26640
120	6292	0	199075	13020
160	6694	0	198376	9394
	Emulsion phase			
40	14796	2061	184278	3356
80	11105	765	190699	1562
120	9095	1.8	194197	481
160	8597	0	195064	559

At excess air factor equals 1 (the stoichiometric ratio), the results seem to be confusing as the concentration of CO increases with jet velocity then decreases again at u_j=160 m/s as shown Fig. 9.b. These confusing results may be explained based on initial concentrations within the three phases. At smallest jet velocity (i.e. 40 m/s), the mass of fuel vapor inside the jet bubble-phase is small because the released fraction of fuel vapor within the jet flare, r_{jfv}, is small (see table 1). The bulk of fuel vapor is released inside the emulsion phase. Consequently, the initial fuel-to-oxygen ratio in emulsion phase is very high (see table 3). Thus a considerable part of oxygen and fuel vapor should be exchanged with the bubble phases to complete the combustion, i.e., the combustion processes mainly turn into mass transfer controlled. Since the mass transfer is not high enough, a considerable part of fuel vapor crosses the bed without reaction (see the final concentration in emulsion phase, table 3). Rising jet air velocity (u_j) increases the fraction of fuel vapor released inside the flare, and hence, the average initial concentration of fuel vapor in the two bubble phases (see Tables 1 and 3). As reported in table 3 the initial fuel-to-oxygen ratio in emulsion phase reduces; however, the mixture is still fuel rich. The rate of fuel vapor oxidation in emulsion phase increases resulting in higher production rate of carbon monoxide. Since the available oxygen is still not sufficient to burn the produced CO, the final result is higher concentration of carbon monoxide and a lower concentration of fuel vapor (see Fig. 9.a and 9.b). These are the cases of jet velocities u_j=80 and 120 m/s. In the case u_j=160 m/s, the initial fuel to oxygen ratio in emulsion phase decreases to such an extent that fuel vapor conversion is completely carried out. Additionally, a considerable part of carbon monoxide burns to carbon dioxide as well. Thus the final concentration of carbon monoxide turns out to be lower.

Liquid Fuel Type

Three different types of petroleum liquid fuel have been studied by the model. They are heavy fuel, diesel and gasoline. Figure 10 shows the axial profiles of CO phase-averaged mole fraction along the bed height. The peaks of carbon monoxide concentration are more pronounced in the cases of gasoline and diesel fuels when compared to the heavy fuel. Moreover, the concentration of CO at the bed surface is considerably lower in the case of gasoline and diesel. This trend should be attributed to the better initial fuel distribution between the emulsion and the bubble phases in the case of gasoline and diesel fuels at the same jet velocity. At u_j= 80 m/s, almost all the injected gasoline and diesel evaporate inside the flare, as the mass fraction of liquid fuel vapor released inside the jet $r_{jfv}=1$ as reported in table 1. Alternatively, the fraction of evaporated heavy fuel is only 0.69 under the same conditions. Increasing r_{jfv} multiplies the fuel vapor content in jet bubble phase (see Eq. 2), which should be oxygen-rich thanks to the fast mass interchange with the distributor bubble phase. Additionally, the carbon monoxide reaction rates are more intensive in the case of gasoline and diesel due to the

higher concentration of H_2O and the better distribution of O_2.

Figures 11.a and 11.b present the influence of jet velocity on the phase-averaged mole fraction of fuel vapor and carbon monoxide at the bed surface for the different fuels. The fuel vapor conversion totally completes inside the bed at lower jet velocity (< 40 m/s) in the case of gasoline and diesel fuel. On the other hand, in the case of heavy fuel vapor concentration, which has significant higher values under the same conditions, gradually diminishes with increasing jet velocity reaching zero at $u_j \approx 100$ m/s.

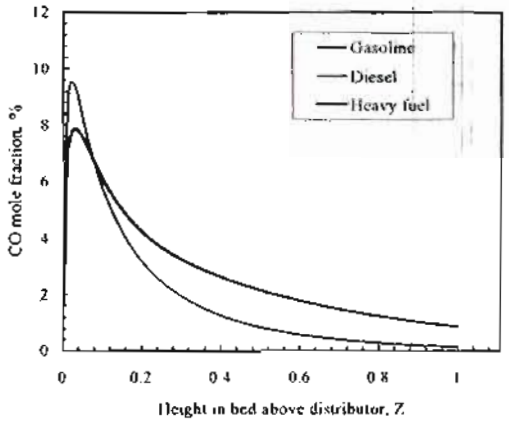

Fig. 10. Axial phase-averaged concentration profile of CO for different fuel types
(u_j=80 m/s, u_o=1.0 m/s, T_B=850°C and EA=1.1)

The carbon monoxide concentration is lower for lighter fuel, as shown in Fig. 11.b. With increasing jet velocity, CO concentration rapidly falls to a low value then levels off, in the case of gasoline and diesel. For the heavy fuel, initially the fuel vapor slowly reduces with jet velocity increase up to u_j=80 m/s then the concentration rapidly decays to nearly the same lower value then levels off, as well, at u_j=170 m/s.

It is worth noting that the axial concentration profiles of carbon monoxide for gasoline and diesel are coincident in Fig. 10. The reported data in table 1 show that the fraction $r_{jfv} = 1.0$, at jet velocity 80 m/s, for the both fuels. Accordingly, the initial concentrations of the phases should be the same for the both fuels. The matching between the two profiles indicates that the model is less dependent on the chemical kinetic. It is appears that chemical reaction is extremely fast when compared to mass transfer. Figures 11.a and 11.b confirm this conclusion where the gasoline and diesel profiles are coincident at $u_j \approx 50$ m/s as the fraction of evaporated vapor inside the jet flare (r_{jfv}) are almost the same. At very high jet velocity (i.e. u_j=170 m/s), the profiles of the three fuel types become coincident including the heavy fuel as it completely evaporates inside the flare ($r_{jfv} \approx 1$) as reported in table 1.

Altogether, these results imply that the combustion processes inside the bed are mainly mass transfer controlled. From this point of view, it may be stated that the assumption of uniform temperature in all phases has a minor impact on the model results.

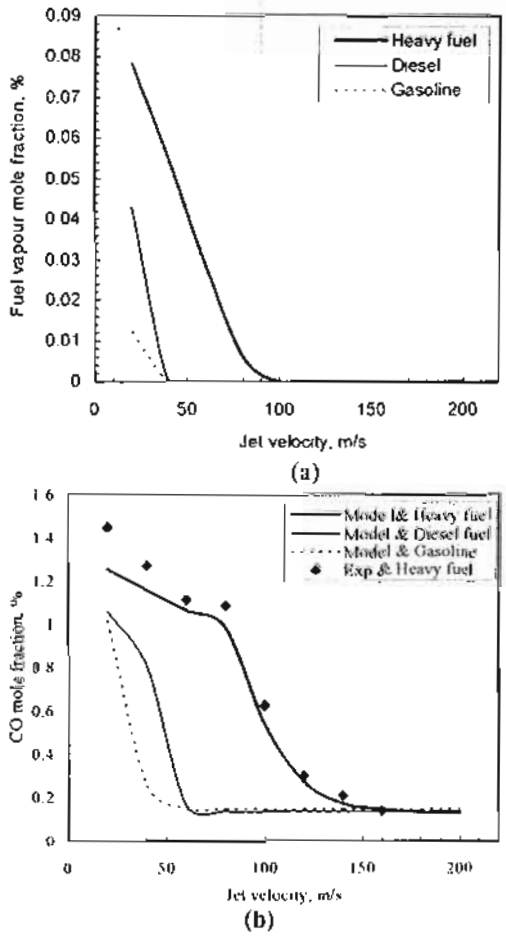

Fig. 11. Phase-averaged concentration of fuel vapor and carbon monoxide at the bed surface for different fuels
(u_o=1.0 m/s, T_B=850°C and EA=1.1)

Comparison with Experimental Results

Steady-state combustion tests have been carried out in an atmospheric bubbling fluidized bed furnace having an inner diameter of 300 mm and a total height of 3300 mm. Details of the apparatus can be found elsewhere (Okasha et. al, 2003). The liquid fuel is introduced at the bottom of the bed by means of an injector, which is vertically mounted at the centerline of the distributor. The liquid fuel is dispersed into the fluidized bed in radial direction via eight nozzles located at 7 cm above the distributor. The nozzles are regularly distributed along the circumference of a 2 cm OD injector with shift angle of 45°. Four of the nozzles discharge in a direction inclined 5° down to horizon whereas the others discharge 30° down to horizon. Silica sand with a narrow size distribution (0.5-0.8 mm) is used as bed material.

The used fuel is a heavy oil (Egyptian mazut), having no oxygen and around 3.2% of sulfur content. Its properties are reported in Tab. 4. The carbon content of the fuel is nearly the same as the model fuel, n-heptane, about 85% on mass basis. The hydrogen content is somewhat less than the model fuel. The fluidization velocity and the bed temperature are fixed at 1.0 m/s and 850°C, respectively.

Table 4. Mazut fuel properties

Physical properties	
Density (at 15.5 °C), kg/m^3	946.1
Moisture content, % by volume	0.2
High heating value, kcal/kg	10338
Low heating value, kcal/kg	9750
Elemental Analysis, (dry, mass basis)	
Carbon, %	84.8
Hydrogen, %	11.6
Sulfur, %	3.2
Ashes	0.4

Design of Experimental Test

A rigorous validation of the model should require measurements of the axial concentration profiles along the bed height that is not possible to be carried out using the current available facility. Instead, the tests are designed to measure the average concentrations close to the bed surface. The static bed height is chosen to be 40 cm that expands to about 60 cm under the chosen operating conditions. The sampling probe of gas analyzer is inserted through an opening in fluidization column found at 60 cm above the distributor close to the expanded bed surface. The probe is movable in radial direction for sampling at different radial positions to have an average value close to the expanded bed surface. The probe position is also verified by direct observation through a glass window.

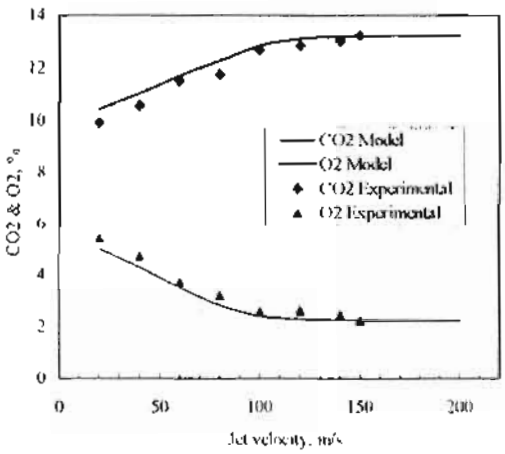

Fig. 12. Comparison between model and experimental results
(Heavy fuel, u_o=1.0 m/s, T_b=850°C and EA=1.1)

The measured results have been plotted in figures 11.b and 12 with model results for comparison. The figures report the average concentration of CO, CO_2 and O_2 at the outlet of the expanded bed. It is noted that there is a good agreement between the experimental and the model results, in particular, at higher jet velocity. The deviation at smaller jet velocity, where the model overestimates the in-bed combustion, could be ascribed to some different reasons. First the model assumes that jet fuel feeding is at very beginning whereas it is actually at about 7 cm above the distributor. However, this shortcoming is partially recovered at higher jet velocity due longer jet penetration with down inclination. The second reason could be that the model overrates the gas interchange coefficient between the jet and

distributor bubble phases. The latter is particularly more significant at the lower jet velocities as the fuel vapor is improperly distributed among the different phases, and in addition, the rate of jet bubble phase is lower. Under these conditions the mass exchange among phases plays the dominant role vs. chemical reaction. On the other hand at higher jet velocity, the fuel vapor is better distributed among the phases and the rate of jet bubble phase is higher. Accordingly, the gas interchange turns into to be less important. Moreover, the longer jet penetration with higher jet velocity should improve the gas mixing at the lower bed zone.

CONCLUSION

A mathematical model that simulates the combustion of liquid fuel in bubbling fluidized bed has been developed. The model is based on the modified two-phase theory of fluidization that regards the bed as three phases: an emulsion phase and two-bubble phases. Two-step fuel reaction has been applied. According to the obtained results the following conclusions may be drawn.

- A new approach is introduced to substitute the gas mixing due to bubbles coalescence with an interchange rate while maintaining the assumption of constant bubble size for simplification. An equivalent mass interchange coefficient is derived based on the growth of bubble size and the probability of coalescence between the jet and distributor bubbles. The relative importance of this coefficient has been evaluated.
- The developed model is able to predict the axial variations in species concentration inside the different phases. The model takes into consideration the chemical reaction in each phase and the interchange of gases among each others. The obtained results showed that the concentrations in the two bubble phases become almost the same in a short distance due to the high estimated mass interchange between the two-bubble phases. The in-bed combustion of fuel included in jet-bubble phase is greatly enhanced thanks to bubbles coalescence.
- The influences of different parameters on combustion performance have been assessed. The jet velocity has a major effect. Increasing jet velocity significantly improves the in-bed combustion thanks to the better distribution of fuel vapor among the three phases. The in-bed combustion enhances with excess air, but on the contrary, it reduces with fluidization velocity. The lighter fuel is burned more efficiently inside the bed than the heavier one under the same moderate injection conditions.
- The results indicate that the combustion processes inside the bed are mainly mass transfer control. From this point of view, it may be stated that the assumption of uniform temperature has a minor impact on the model results.
- The comparison between the model and experimental results shows a good agreement, especially at the higher jet velocities.
- The model results yield highly efficient in-bed combustion (i.e. low concentrations of fuel vapor and CO at the bed surface) when the fuel is initially well distributed between the emulsion and the jet bubble phase. In the experimental work the liquid fuel was injected by eight nozzles that should result in well distributed fuel over the bed cross sectional area as well. This looks a confirmation that an even distribution of injected liquid fuel inside the bed is the most important factor for highly efficient in-bed combustion.

REFERENCES

1. S.C. Saxena and K. Jotshi, Prog. Energy Combust. Sci. 20 (1994) 281-324.
2. D. Barker, B. Beacham, Proc. Of the Inst. Of Fuel Inter. Conf., London (UK), (1980) I-A3.
3. B. Beacham and A. R. Marshall, Journal of Institute of Energy, June, (1979) 59-64
4. R. Legros, C.J. Lim, C.M.H. Bretreton and J.R. Grace, Fuel 70 (1991) 1465-1471.
5. North B., Eleftheriades C., Engelbrecht A., 15th Int. Conf. on Fluidized Bed

Combustion, ASME, Savannah, USA, (1999) Paper No. FBC99-0017.
6. Zhang J., Lu D.Y., Anthony E.J., 16th Int. Conf. on Fluidized Bed Combustion, ASME, Reno Nevada, USA (2001) paper FBC01-0093.
7. Okasha F., El-Emam S. H. and Mostafa, H. K, "The Fluidized Bed Combustion of heavy liquid fuel (Mazut)", Experimental Thermal and Fluid Science Journal, April 2003, Volume 27, Issue 4, pp. 473-480.
8. Stubington J.F. and Davidson J.F., AIChE Journal,1981, 27,59.
9. Borodulya V.a., Dikalenko V.I., Dobkin S.M. and Markevich I.I., Heat Transfer Research, 1992, 24,832.
10. Miccio, F., Miccio, M. and Olivieri, " A study on Bubbling Bed Combustion of Gasoil", G., Proc. Of the 16th International Conference on FBC, 2001, FBC01-0178, Reno, USA.
11. Faravelli, T., Frassoldati A., Ranzi A., Miccio F. and Miccio, M, "Modeling Homogeneous Combustion in Bubbling Beds Burning Liquid Fuel", Proc. Of 17th Int. FBC Conf., ASME, 2003, paper 133.
12. Faravelli, T., Frassoldati A., Ranzi A., Miccio F. and Miccio, M, "Modeling Hydrocarbon Oxidation and Pollutant Formation in FBC of Liquid Fuels", Proc. Of the 11th int. Conf. On Fluidization, 2004, EE4, Naples, Italy.
13. Scala F., Miccio F. and Miccio, M.,"A 1-D Zone Model for the Axial Burning Profile of Liquid Fuels in Bubbling Fluidized Beds", Proc. Of the 11th int. Conf. On Fluidization, 2004, Naples, EE11, Italy.
14. Miccio F, and Okasha F., "Fluidized Bed Combustion and Desulfurization of a Heavy Liquid Fuel", Chemical Eng. Journal, 2004, Vol. 105/3, pp 81-89.
15. Okasha F. and Miccio M., "Modeling of Wet Jet in Fluidized Bed" submitted to Chemical Engineering Science Journal.
16. Hilligardt and Werther J., in Proc. 3rd World Cong. Of Chem.Eng., Tokyo, 1986. Werther J., in Fluidization IV, Kunni D., and Toei R., p. 93, Engineering Foundation, , 1983, New York.
17. Kunii, D., and Levenspiel, O., "Fluidization Engineering", Butterworth-Heinemann, Second Edition, 1991.
18. Massimilla, L., "Gas Jet in Fluidized Beds", (2nd Ed., Edited by Davidson, J. F., Clift, R. and Harrison, D.),pp. 133-172, Academic Press, New York, 1985.
19. Buevich Yu. A. and Minaev G. A., Inzh Fiz. Zh. 30, (1976), No. 5, 825-833.
20. Nguyen, X. T. and Leung L. S., Chem. Eng. Sci., (1972), 27, 1748-1750.
21. Yates, J. G., Rowe P.N. and Cheesman D. J., (1984), AIChE J., 30, 890; Yates, J. G., Bejek V. and Cheesman D. J., (1986), in Fluidization V, Ostergaard K. and Sorensen A., eds, p. 79, Eng. Foundation, 1986, New York.
22. Cai P., Schiavetti M., De Michele G., Grazzini G. and Miccio M., "Quantative Estimation of Bubble Size in PFBC", Powd. Tech. , 1994, Vol. 80, pp. 99-109.
23. Davidson J. F. and Harrison O, "Fluidized Particles", Cambridge Univ. Press London, 1963.
24. Clift, R., and Grace, L. R., "Continuous Bubbling and Slugging", (2nd Ed., Edited by Davidson, J. F., Clift, R. and Harrison, D.),pp. 73-132, Academic Press, New York, 1985.
25. Borman G. and Ragland K. (1998), "Combustion Engineering", McGraw-Hill.
26. Westbrook, C. K., and Dryer, F. L., "Chemical Kinetic Modeling of Hydrocarbon Combustion", Prog. Energy Comb. Sci., 1984, vol. 10, pp. 1-57, 1984.
27. Howard J. B., William G. C. and Fine D. H., "Kinetics of Carbon Monoxide Oxidation in fast flame gases", 14th Symp. Inter. On Combustion, Pittsburgh (Pennsylvania), The combustion institute, (1973), pp. 973-986.
28. Philippek C., Knobig T, Schnfelder H., Werther J., "Nox Formation and Reduction During Combustion of Wet Sewage Sludge in the Circulating Fluidized Bed-Measurement and Simulation", 14th International Conference on FBC, 1997.